# Tsunami Radiation Pattern in the Eastern Mediterranean

Lyuba Dimova, Reneta Raykova

*Department of Meteorology and Geophysics, Faculty of Physics, Sofia University "St. Kliment Ohridski", 5 James Bouchier Blvd., 1164 Sofia, Bulgaria*

**Abstract.** The region of the Eastern Mediterranean suffered by strong earthquakes generating tsunami waves. The geological and geophysical structure beneath this area is very complicated and remains unclear. Definitely one of the most active seismic zones is the Hellenic arc situated near the boundary between the African and the Aegean tectonic plates. In this study we examined the tsunami radiation pattern from different seismic sources in the Eastern Mediterranean. We performed simulations by means of the numerical code UBO-TSUFD in approximation of a shallow water theory using finite difference technique. The tsunami propagation is estimated by two equations, continuity equation and the momentum conservation, and suitable boundary conditions. The distribution of maximum water elevation and the water column inland are calculated and presented. Computed synthetic mareograms showed the impact on the coast in some locations close to big cities.

**Keywords**: tsunami, seismic sources, numerical simulations, Eastern Mediterranean.

## 1. INTRODUCTION

The term tsunami comes from the Japanese language ''tsu'' means harbor and ''nami'' means wave. Tsunamis are gravity waves that propagate across the water basins. They are caused by earthquake, submarine or subaerial landslide, caldera collapse, volcano eruption or even impacts.

We focused this study in the modeling of earthquakes-induced tsunamis. A tsunami in the deep ocean has a wavelength of about 200 kilometers and travel with speed more than 800 km/h. As the tsunami approaches the coast and the waters become shallow, wave shoaling compresses the wave and its velocity slows below 80 km/h and its wavelength decrease to less than 20 kilometers and its amplitude increase. The tsunami have a greater periods than the beach waves, so the "tsunami window" covers waves of 70, 200, 500 or even 2000 s period, unlike the beach waves, tsunami arrive and may continue to flow in for several minutes (Ward, 2001). Tsunami eigenfunctions describe wave motion of a particular frequency (see Fig. 1). The description of waves with length $\lambda$ in oceans of depth $H$ commonly include two simplifications: a long wave approximation ($\lambda >> H$, $1/k >> H$, where $k$ is wavenumber) and a short wave approximation ($\lambda << H$, $1/k << H$).

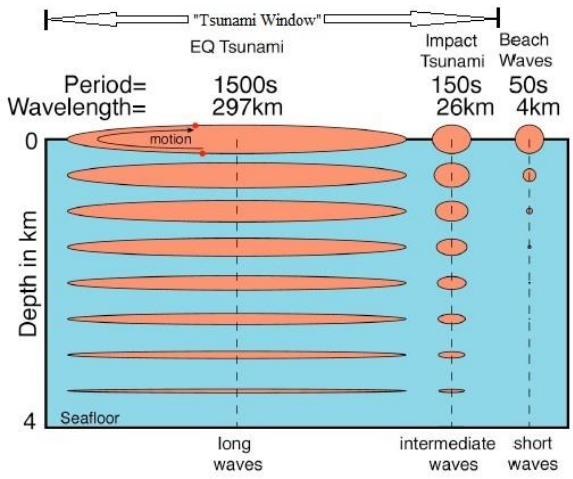


**Fig. 1** Tsunami Eigenfunctions in a 4km deep ocean (modified from Ward, 2001).

The long wave theory predicts non-dispersive wave propagation with velocity $c(\omega) = u(\omega) = \sqrt{gH}$ ($c$ is phase velocity, $u$ is

group velocity, $\omega$ is frequency and $g$ is gravity acceleration), while the short wave approximation predicts dispersive wave propagation with velocity $c(\omega) = 2u(\omega) = \frac{gT}{2\pi}$, where $T$ is wave period.

## 2. MATERIALS AND METHODS

Numerical simulations are useful tools in tsunami research since they are used to reconstruct recent and historical events. We used methodology that is separated in two steps: (1) computing the coseismic deformation, as a function of the fault geometry and the ground elastic parameters, displacements due to an elastic dislocation obtained by the analytical formulas of Okada (1985, 1992); (2) computing the propagation of tsunami waves and their effects on the coasts. The theory for tsunami propagation is based on two conservation laws, in case of no energy dissipation, namely the mass conservation (continuity equation) and the momentum conservation, and on appropriate boundary conditions. The numerical code UBO-TSUFD has been developed at the University of Bologna, Italy and it is based on the non-linear shallow water theory in a Cartesian frame (Tinti and Tonini, 2013). The bottom friction is taken into account and the code uses a staggered grid by mean of an explicit leapfrog finite-difference method.

## 3. RESULTS

We studied four tsunamigenic zones in the area of the Eastern Mediterranean (Fig. 2). The faults, generating earthquakes, are obtained from databases compiled in SHARE - The European Database of Seismogenic Faults, GreDaSS and DISS - The Database of Individual Seismogenic Sources (Basili et al., 2008).

The geometry of the faults (see Table 1) is calculated by the regressions proposed by Mai and Beroza (2000) and Wells and Coppersmith (1994).

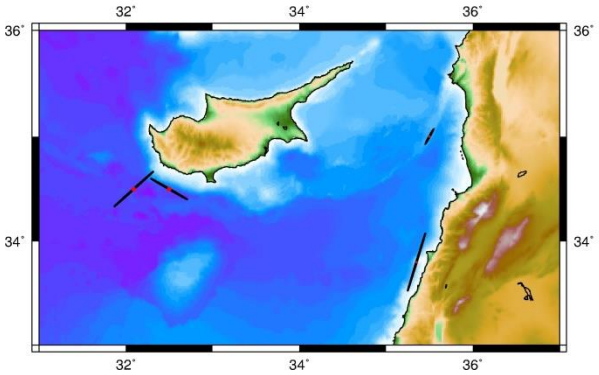


**Fig. 2** Positions of the selected hypothetical seismic sources.

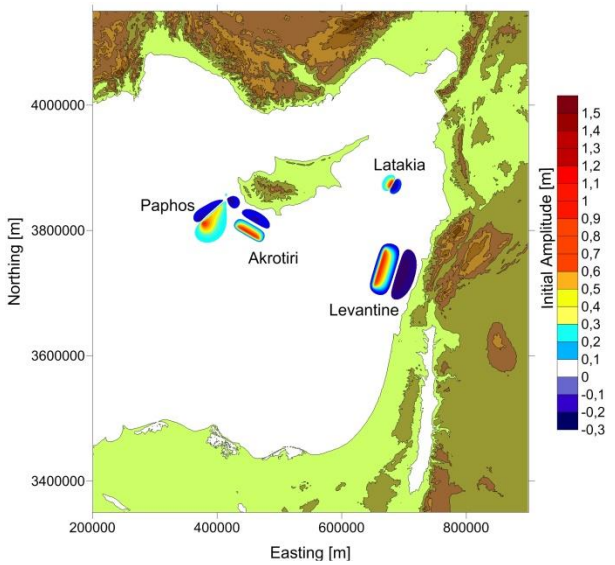


**Fig. 3** Initial displacements of the hypothetical seismic sources.

**TABLE 1.** Fault zones and selected fault parameters.

| Fault Zone / Fault Parameters | Akrotiri | Paphos | Latakia | Levantine |
|---|---|---|---|---|
| **Mw** | 7.2 | 7.4 | 6.5 | 7.5 |
| **L (km)** | 45 | 56 | 17 | 65 |
| **W (km)** | 20 | 26 | 10 | 30 |
| **Slip (m)** | 3.0 | 3.5 | 1.5 | 4.0 |
| **Strike (degree)** | 300 | 48 | 209 | 17 |
| **Dip (degree)** | 30 | 77 | 75 | 30 |
| **Rake (degree)** | 90 | 170 | 85 | 90 |
| **Depth (m)** | 3500 | 3000 | 2500 | 4000 |
| The depth corresponds to the Upper Border Middle Point of the faults. | | | | |

Focal mechanism solutions are in accordance with recent earthquakes and the geological settings in the region. Initial displacements shown in Fig. 3 are calculated by Okada`s formulas that result from the analytical integration of the double-couple point-source solutions over a rectangle of length L and width W. The properties of the grid used in these simulations are as follow:

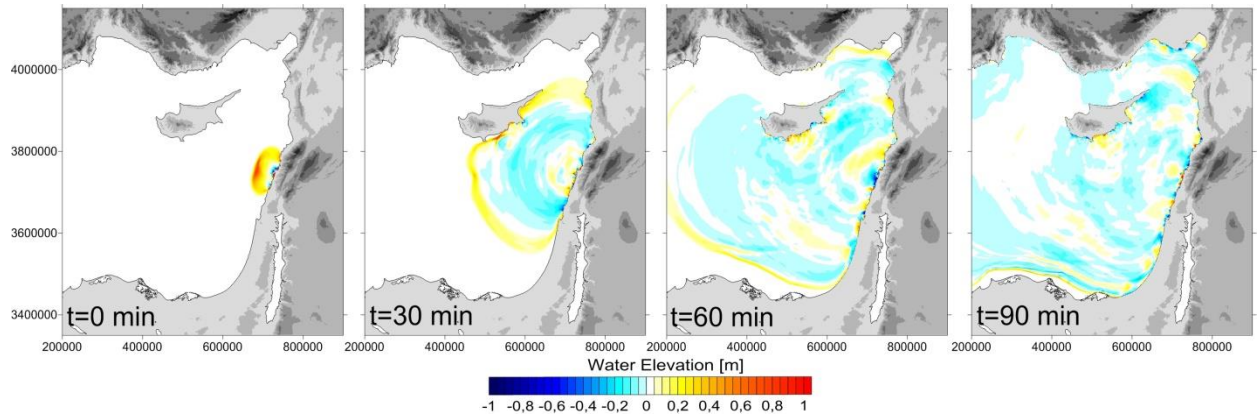


**Fig. 4** Tsunami scenario related to Levantine fault zone (snapshots of the computed water elevation fields are at 30-minute intervals after the earthquake).

grid step 500 m, total number of nodes is 2243001, a time step for every cell is 1.5 s. Topography and bathymetry data are taken from GEBCO.

The wave propagation of tsunami waves generated by hypothetical seismic source in the region of the Levantine coast is presented in Fig. 4. Waves reached in 20 to 30 minutes the southeastern coasts of Cyprus with amplitudes around 1.0 m. The first positive wave hits the coasts of the Turkish provinces Adana and Hatay in 60 minutes. The estimated maximum water elevation near the coast of Meydan and Latakia is +0.8 m and +1.4 m respectively. In one hour the city of Alexandria experiences waves of height around 0.4 m, while Tel-Aviv is hit in 30 minutes after the earthquake onset by positive waves with amplitudes around 0.4 m.

The code calculated the fields of maximum water elevation for every hypothetical seismic source. Fig. 5 and Fig. 6 represent the tsunami radiation pattern as maximum water elevations for four sources.

Fig. 6 and Fig. 7, show that Akrotiri and Levantine fault zones have the largest impact on the coast of Egypt (Alexandria and surrounding area). Paphos seismic source has some impact near Antalya (Turkey) and Peninsula Sinai even with the strike-slip mechanism of the earthquake.

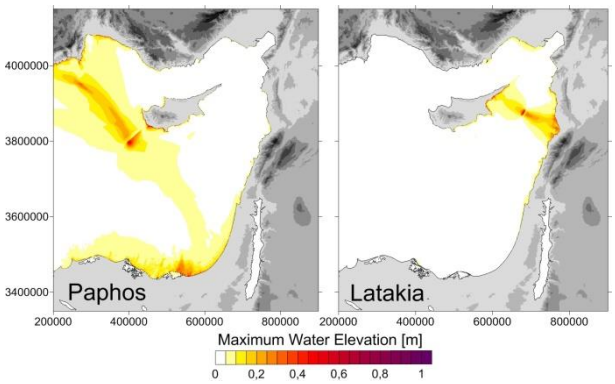


**Fig. 5** Maximum Water Elevation for Paphos and Latakia tsunamigenic sources.

The highest tsunami risk for southeastern Cyprus and Levantine countries involve the Levantine seismic source. Latakia fault zone produce waves with amplitudes around 0.5 m near Tartus (Syria).

We calculated synthetic mareograms near the biggest cities of each region. The graphical

record produced by these simulated mareographs, shows variations in the sea level depending on the time elapsed from the simulated onset. The synthetic mareograms play an important role for a quick system of tsunami warning since they can be constructed before the event occurs.The position of several synthetic mareograms is shown in Fig. 8. The depth of these locations varies between 0 and -20 m.

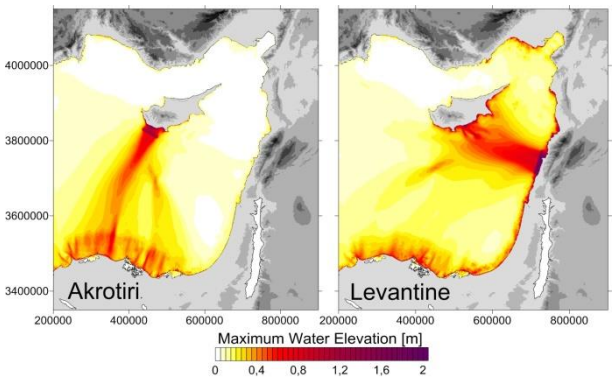


**Fig. 6** Maximum Water Elevation for Akrotiri and Levantine tsunamigenic sources.

The highest tsunami risk for southeastern Cyprus and Levantine countries involve the Levantine seismic source. Latakia fault zone produce waves with amplitudes around 0.5 m near Tartus (Syria).

We calculated synthetic mareograms near the biggest cities of each region. The graphical record produced by these simulated mareographs, shows variations in the sea level depending on the time elapsed from the simulated onset. The synthetic mareograms play an important role for a quick system of tsunami warning since they can be constructed before the event occurs.The position of several synthetic mareograms is shown in Fig. 8. The depth of these locations varies between 0 and -20 m.

Fig. 9 presents an example of a tsunami records near four of the major cities in the area. The colors of the four graphs presented in Fig. 9 correspond to hypothetical seismic sources as follow: Akrotiri-black, Paphos-blue, Latakia-green and Levantine-red. In the case of Paphos city the highest impact comes from Akrotiri hypothetical seismic source (M=7.2) since the mechanism of the earthquake is reverse faulting. The vertical component of the water shift is biggest. Latakia hypothetical seismic source produces quite large amplitudes for the city of Tartus, although the magnitude is 6.5. The third graph (Beirut) shows high jump of around 6.0 m, due to Levantine hypothetical seismic source (M=7.5). After the first wave with height of 2.0 m, a negative onset follows with amplitude of -4.0 m with receding of the sea.

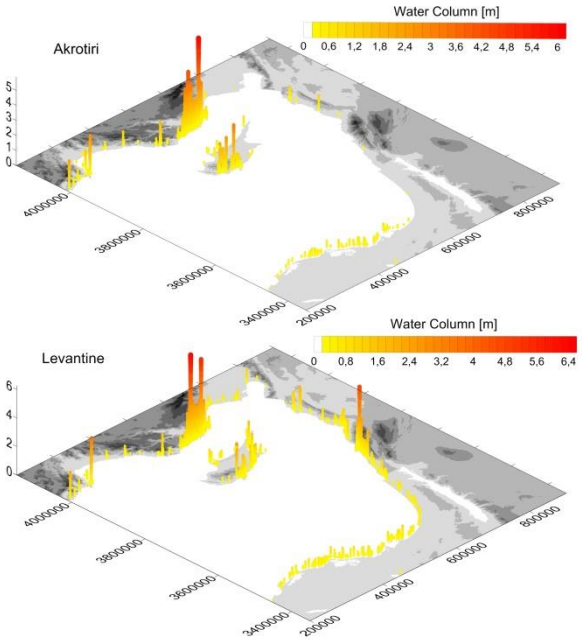


**Fig. 7** Water Column Inland.

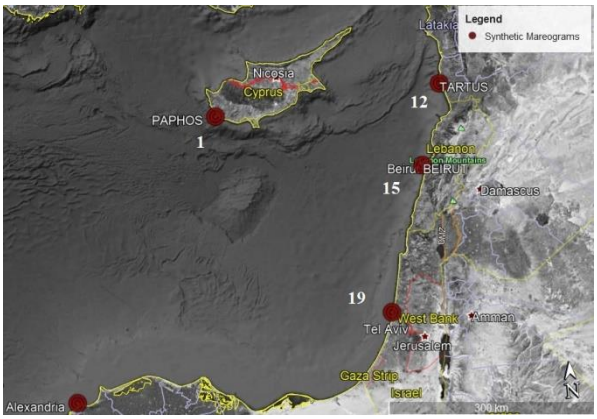


**Fig. 8** Positions of the selected synthetic mareograms.

The impact for Beirut from the other three sources is negligible compared to this one. The highest tsunami impact for the city of Tel-Aviv comes from the hypothetical seismic source Levantine. Calculations show that the largest deviations from the sea level are not associated with the first wave arrival but afterwards (2 hours and 20 minutes). Akrotiri and Paphos hypothetical sources have small impact on the coast of Tel-Aviv, around 0.2 m.

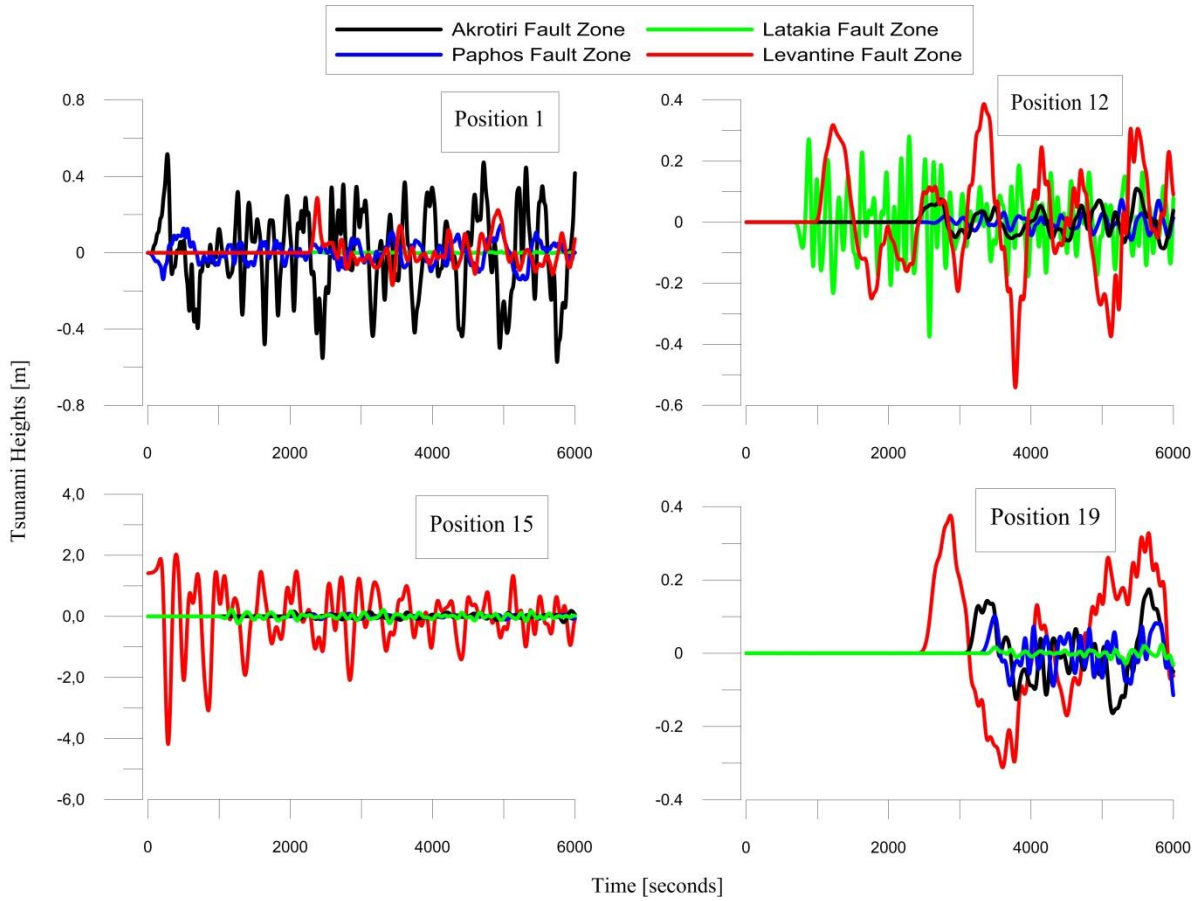


**Fig. 9** Synthetic Mareograms: 1-Paphos (Cyprus), 12-Tartus (Syria), 15-Beirut (Lebanon) and 19-Tel-Aviv (Israel).

## 4. COMMENTS AND CONCLUSIONS

We examined four scenarios of earthquake-induced tsunamis in the Eastern Mediterranean. We take into account magnitudes equal to or slightly larger than the strongest event known to have occurred in historical times in each region. All sources are situated close to the coast, which is a typical feature of most sources of the Mediterranean Sea. Some coasts are reached by tsunami in a very short time, less than 20-minute. The need of tsunami early warning system in short time period in the region of the Eastern Mediterranean is of great importance since it can prevent some losses and victims caused by future tsunami impacts. The highest amplitudes are not necessarily associated with the first wave arrival, furthermore sea-level oscillations remain significant for several minutes to hours after the earthquake and this require more attention in tsunami modelling and tsunami warning.

## ACKNOWLEDGEMENTS

The presented work is supported by project 80-10-21/19.04.2017 “Numerical modelling of tsunami waves in the region of Aegean Sea”

funded by the SCIENTIFIC RESEARCH FUND OF SOFIA UNIVERSITY.

## REFERENCES

Basili, R., Valensise, G., Vannoli, P., Burrato, P., Fracassi, U., Mariano, S., Tiberti, M.M. & Boschi, E., 2008. The Database of Individual Seismogenic Sources (DISS), version 3: summarizing 20 years of research on Italy's earthquake geology, *Tectonophysics*, 453, 1, 20-43.

Mai, P.M. & Beroza, G.C., 2000. Source scaling properties from finite-fault-rupture models, *Bull. seism. Soc. Am.*, 90, 3, 604-615.

Okada, Y., 1985. Surface deformation due to shear and tensile faults in a half space, *Bull. seism. Soc. Am.*, 75, 4, 1135-1154.

Okada, Y., 1992. Internal deformation due to shear and tensile faults in a half space, *Bull. seism. Soc. Am.*, 82, 2, 1018-1040.

Tinti, S. & Tonini, R. 2013. The UBO-TSUFD tsunami inundation model: validation and application to a tsunami case study focused on the city of Catania, Italy, *Nat. Hazards Earth Syst. Sci.*, 13, 1759-1816.

Ward, S., 2010. Tsunami, *In: Encyclopedia of Solid Earth Geophysics*, Springer,1-18.

Wells, D.L. & Coppersmith, K.J., 1994. New Empirical Relationships among Magnitude, Rupture Length, Rupture Width, Rupture Area, and Surface Displacement, *Bull. seism. Soc. Am.*, 84, 4, 974-1002.